SUMO User Conference 2026

TIBconferencesession

TIB-OP_will_set_DOI

Published: 2026-XX-XX

Enabling Non-Lane-Based Cycling Behavior for Mass Bicycle Traffic Flow Simulation in SUMO

Ying-Chuan Ni[1], Thomas Ramseier[1], Junzhe Cao[1], Anastasios Kouvelas[1], and Michail A. Makridis[1]

[1]Traffic Engineering Group, Institute for Transport Planning and Systems, ETH Zurich, Zürich, Switzerland

*Correspondence: Ying-Chuan Ni, ying-chuan.ni@ivt.baug.ethz.ch

Abstract. Studies have increasingly used microscopic traffic simulation to evaluate the efficiency of bicycle infrastructure in multi-modal urban road networks. However, compared with models for motorized vehicles and pedestrians, state-of-the-art bicycle movement models in traffic simulation tools still fall short in reproducing realistic cycling behavior and therefore require substantial improvement. This work implements a non-lane-based bicycle simulation model in SUMO. Lateral movements, including overtaking and aligning behavior, are governed by a decision-making mechanism developed from insights obtained through naturalistic observations. The model computes both cyclists' lateral movement distance and longitudinal acceleration and integrates them into the sublane environment in SUMO. The proposed model is capable of (i) achieving staggered queue formation through a modified gap function based on a hexagonal bicycle representation, (ii) introducing efficient queueing behavior that enhances lateral space utilization in bicycle flow, (iii) avoiding collisions by predicting the future positions of the ego-cyclist and its surrounding cyclists, and (iv) accounting for human factors by incorporating cyclists' decision-making frequency and reaction time lag. We verify the model by analyzing queue formations and intersection capacities in signalized bicycle lane scenarios with varying lane widths. Future work will focus on calibrating the model parameters using real-world bicycle trajectory data. The proposed model is expected to improve the reproduction of bicycle traffic flow dynamics under conditions of mass cycling demand.

Keywords: Bicycle Flow, Cycling Behavior, Decision-Making, Human Factors, Microscopic Traffic Simulation, Non-Lane-Based Movement, Reaction Time Lag, Staggered Queue Formation, SUMO, Sublane Model

1. Introduction

Cycling is considered a sustainable and efficient transport mode that can contribute to reducing emissions and potentially alleviating traffic congestion in urban road networks. Therefore, major cities around the world have been allocating more urban road space

to bicycles [1]. As cycling demand increases, a traffic simulation model tailored for bicycles is crucial for transport planners and traffic engineers to examine the quality of bicycle lane networks [2]–[4]. As experimentally shown in Wierbos et al. [5], the width of the bicycle lane is one of the factors that influence the aggregated bicycle flow performance. Therefore, it is important to design bicycle lane networks and evaluate multi-modal urban traffic management strategies with the help of a reliable bicycle traffic simulation tool.

In recent years, studies have begun to use Simulation of Urban MObility (SUMO) [6], an open-source traffic simulation package, to simulate microscopic bicycle flow. Grigoropoulos et al. [7] used SUMO to simulate the effect of a pilot bicycle corridor in the city of Munich with advanced traffic signal control strategies that consider cycling demand. Fulton et al. [8] evaluated the traffic efficiency of an envisioned bicycle lane network for the city of Zurich by running the simulation with SUMO. However, the model is not exclusive to bicycles. It is an adaptation of longitudinal following and lane-changing models designed for cars, such as the intelligent driver model (IDM) and SL2015. That is, bicycles are modeled as “slow cars” with the current setup in SUMO.

Roosta et al. [9] reviewed the current bicycle traffic flow simulation function in SUMO. Several drawbacks have been highlighted. The major points include (1) lack of stochasticity in longitudinal following and lane-changing behavior mechanism, (2) rectangular-shaped representation of bicycles, and (3) conservative behavior at unsignalized intersections, etc.

Several research attempts have sought to improve the bicycle simulation function in SUMO. Kaths and Roosta [10] and Kaths [11] developed *CyclistModel*, an approach that integrates the concept of the desire line and an adapted social-force model. It enables simulation of flexible two-dimensional movement while mainly maintaining the longitudinal travel direction. However, the model has only been applied to single intersections but has not yet been extended to large urban road networks that contain complex road geometries and various traffic rules.

Similar to *CyclistsModel*, we believe that non-lane-based bicycle movement lies between the single-file longitudinal following dynamics exhibited by cars and the two-dimensional pedestrian motion. In addition, the movement is largely influenced by cyclists’ behavioral heterogeneity. This work aims to implement the model proposed by Brunner et al. [12], which mimics the decision-making process in cyclists’ operational behavior to better account for human factors, in SUMO. Some modifications are also introduced to the original model so that it can be easily integrated into the existing simulation setup in SUMO.

Section 2 introduces the details of the developed model, while Section 3 explains how the model can be integrated into the current SUMO setup. Several test scenarios are shown in Section 4. Finally, the last section mentions all the extensions planned for the model in the near future.

2. Non-lane-based bicycle traffic simulation model

In this work, several modifications to the original model proposed by Brunner et al. [12] are introduced. This section recapitulates the original model structure and explains the changes in the new version. In addition, we include the reaction to traffic lights in the model to simulate interrupted bicycle flow in urban road networks.

2.1 Hexagonal-shaped bicycle representation

To enable staggered queue formation and more congested traffic state for bicycle flow, a commonly-discussed approach is to adopt a diamond shape to represent individual cyclists instead of a rectangular shape used for cars. Falkenberg et al. [13] can be considered one of the earliest attempts that model bicycles with a diamond-shape. Gavriilidou et al. [14] also proposed a choice modeling approach to simulate cyclists' diamond-queueing process before a stop line. Wierbos et al. [15] further investigated the effect of different queue formations on the queue discharge rate of bicycle flow. In the original model of this work [12], the diamond-shaped representation was also used.

In this new version, we introduced a hexagonal-shaped representation of bicycles, as shown in Figure 1, to always maintain the width of the bicycle frame. The span between a cyclist's arms is reflected by the widened width in the middle of the hexagon. It is suggested that the bicycle frame covers 0.35 m of the width, while another 0.65 m is required to include cyclists' arm span.

This unique shape representation affects the calculation of the gap between two cyclists. The gap depends on the relative lateral position of the leading cyclist to the ego-cyclist. The shortest longitudinal distance between the hexagons of two cyclists is the gap that would be used when determining the longitudinal acceleration. By adopting this shape and the adjusted gap, cyclists can queue more closely in a staggered formation.

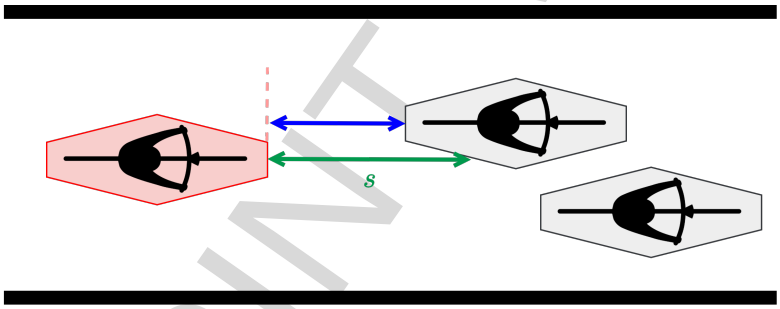

Figure 1. *Bicycle shape representation and gap calculation (green arrow: gap calculated using the hexagonal shape, blue: gap calculated using the rectangular shape)*

2.2 Efficient queueing behavior

In urban traffic flow, interrupted stop-and-go movements occur frequently due to traffic signal control. For bicycle traffic that has great lateral flexibility, when approaching a queue, cyclists tend to move laterally to reach the most downstream longitudinal position. As a result, the queue discharge rate and jam density both increase, making the bicycle flow more efficient.

To simulate this kind of behavior explicitly, a lateral queue space finding behavior is proposed. It is triggered when the gap is larger than a certain threshold. When performing a queueing action, cyclists would check if the longitudinal gap increases when moving laterally toward the sublanes on the opposite side in relation to the direct leader. To move further downstream, the sublane with the longest gap before it begins to decrease would become the ego-cyclist's desired lateral position. Figure 2 illustrates how the ego-cyclist selects the queue position given its current lateral position. It is worth highlighting that the two positions in the figure keep the same final gap with the leader but result in different space utilization efficiency.

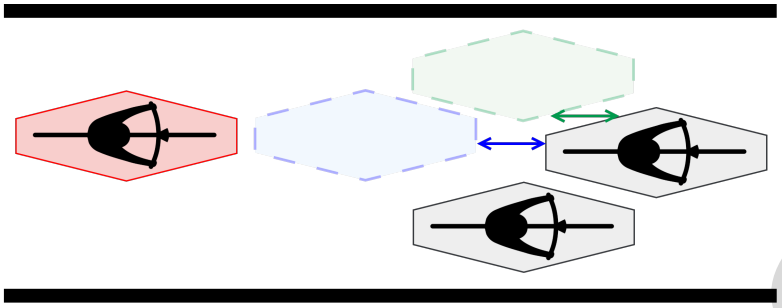

Figure 2. *Efficient queueing behavior (green: queue position found through efficient queueing behavior, blue: queue position without efficient queueing behavior)*

2.3 Non-lane-based collision avoidance mechanism

To prevent collisions, a non-lane-based collision avoidance mechanism must be performed after the desired lateral position is found. This is applied whenever the action determined contains a lateral movement, such as the efficient queueing behavior and overtaking or aligning in uninterrupted flow conditions.

The ego-cyclist predicts the future positions of itself and the surrounding cyclists, including those in front of it within the look-ahead distance and those behind it within the look-back distance, using the fundamental kinematic equation of motion with constant acceleration, as written in Equation 1. x, v, and a are the position, speed, and acceleration along the longitudinal or lateral axis. For the prediction of lateral positions, it is worth noting that the lateral acceleration is a constant value in SUMO. More details about parameter settings are explained in the next section.

Based on the predicted future positions, the ego-cyclist then checks if its future safety region (SR) encroaches any of the surrounding cyclists. The definition of SR is explained in the next subsection. Figure 3 illustrates a situation in which the future SR of the ego-cyclist encroaches on the surrounding cyclist so that the overtaking behavior would not be performed.

$$x_{i+1} = x_i + v_i \cdot t + \frac{1}{2} \cdot a_i \cdot t^2 \tag{1}$$

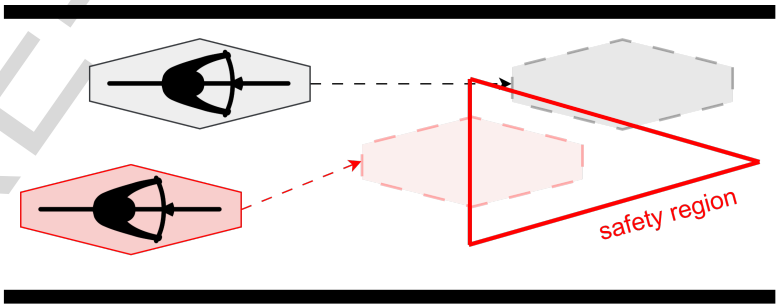

Figure 3. *Detected potential collision in a future time step*

The collision avoidance mechanism is performed for every future simulation step until the minimum time-to-collision (TTC) value. If a potential collision is detected in one of the future steps, the lateral movement would be canceled.

2.4 Mental-layer decision-making process

Cyclists' operational-level behavior is divided into the mental- and physical-layers. In the mental-layer, cyclists' intended action is decided based on their own state and the surrounding condition. In addition, the lateral movement distance would also be determined in this layer.

We show how the decision is made by checking all the conditions in Figure 4. Actions are divided into four different categories. Cyclists would check sequentially (1) if they should remain in a standstill state, (2) if they are approaching a stop line or queue, (3) if they are riding at low speed (slower than the low speed threshold), still discharging, or within an intersection (junction). Otherwise, (4) they are moving in the uninterrupted flow mode.

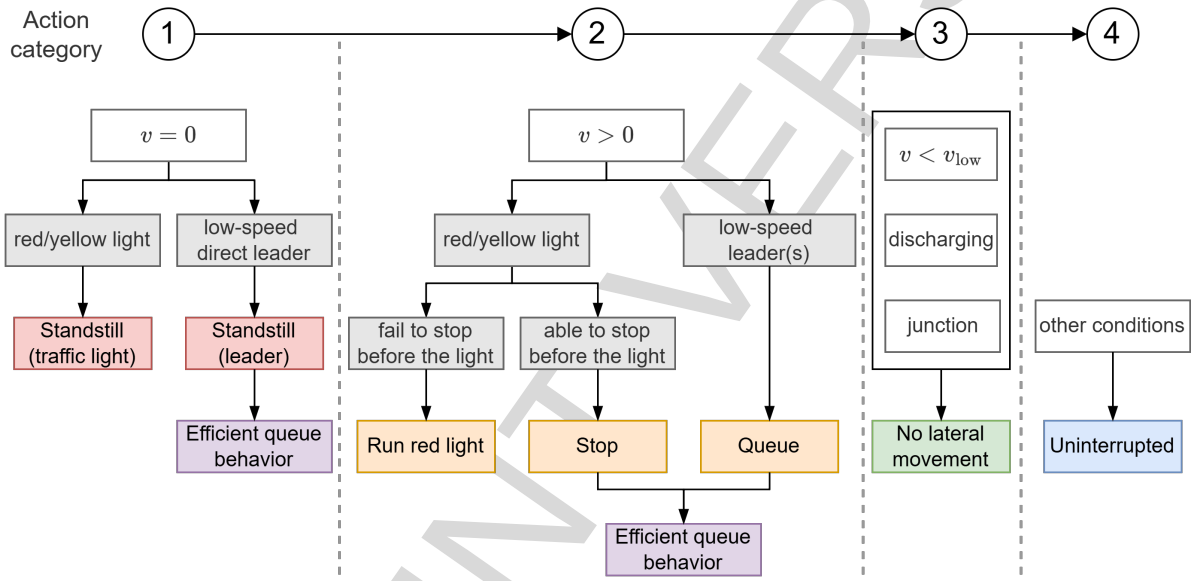

Figure 4. *Decision-making process for the action to be performed (The traffic light state is only checked when there is no leader before the traffic light. The condition "low-speed direct leader" indicates that the direct leader is in standstill or low-speed mode, while "low-speed leader(s)" checks if there is at least one leader that is in standstill or low-speed mode.)*

Cyclists in complete standstill first determine if any action needs to be performed given the traffic light color or the direct leader's state. For a cyclist who is in complete standstill right before the stop line and keep a sufficiently close distance to it, no action is needed when the light is still red. Similarly, a cyclist queueing behind a leader would check if the gap is smaller than the threshold value. If so, no action would be performed. Unlike a standstill cyclist right before the stop line, if there is a downstream queue space available, the cyclist queueing behind a leader would perform efficient queueing behavior and move to the desired lateral position accordingly, as explained in Section 2.2.

In the next action category, cyclists perceive a stop line or standstill queue that overlaps with them on the lateral plane within their look-ahead distance. For those approaching the stop line, they would first check if they can successfully stop (decelerate to zero speed) before the stop line. Otherwise, the run-red-light action would be performed. They then start to slow down to standstill before the stop line or queue behind the direct leader. No lateral movement would be considered unless a downstream queue space is found through the efficient queueing behavior.

If cyclists are moving at low-speed without approaching a stop line or queue, this means that they are in a stabilizing or discharging mode [16]. In these conditions, they would not perform any extra lateral movement in the simulation. In addition, if a cyclist is within an intersection, lateral movement is also disallowed. Such simplification is designed to avoid causing disruptions behind the ego-cyclist in unnecessary conditions.

Finally, in uninterrupted flow conditions, the similar behavior logic proposed in the original model [12] is used to determine the desired lateral position for overtaking maneuvers. Cyclists within the look-ahead distance are first categorized based on their current longitudinal speed. The ego-cyclist finds the most probable lateral space that is larger than its SR width to overtake slow cyclists within the look-ahead distance. In this model, the SR is an area that cyclists tend to keep clear to avoid collision. Its size is influenced by the longitudinal speed. A faster cyclist would require a longer and wider clear space around itself. Unlike the rectangular-shaped SR in Brunner et al. [12], the SR becomes a triangular area in the model, as shown in Figure 5. l_b and w_b denote the length and width of a cyclist, respectively. α and β are the SR size coefficients. While the SR length solely depends on the longitudinal speed v, the SR width is constrained by a maximum factor $\delta^{\max}$. This is similar to the lateral model setting in PTV Vissim [17]. Compared to the original setup, the triangular SR shape aligns better with the newly-proposed hexagonal-shaped representation of cyclists and potentially allows the bicycle flow to reach a higher density in congested conditions because of the smaller area requirement.

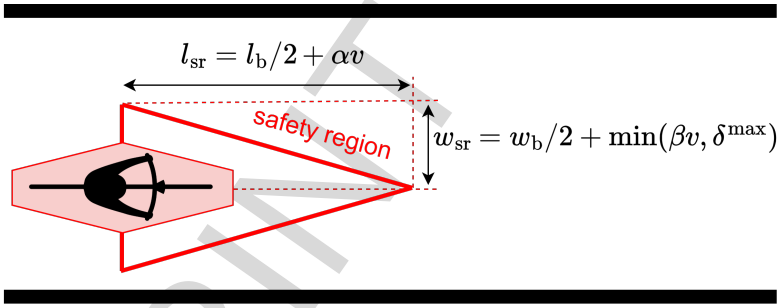

Figure 5. *Safety region size*

Figure 6 illustrates a searching behavior for the overtaking lateral space. The ego-cyclist selects the cyclist to be overtaken by checking the farthest available lateral space within its look-ahead distance. The lateral space that is wider than the required width would be chosen, while the required width w' depends on the longitudinal speed of the cyclist that is about to be overtaken v_{overtake}, as written in Equation 2. ϵ is the speed difference threshold. To overtake, the ego-cyclist needs to be faster than $v_{\text{overtake}} + \epsilon$. Accordingly, the desired lateral position and hence the lateral movement distance are determined.

$$w' = w_\mathrm{b} + \min(\beta \cdot (v_{\text{overtake}} + \epsilon), \delta^{\max}) \tag{2}$$

If there is no incentive for overtaking, meaning that there is no slow cyclist within the look-ahead distance, a right-aligning behavior is performed. After the action decided, as in the efficient queueing behavior, the collision avoidance mechanism is also performed here to prevent causing any collision with surrounding cyclists or strong disruption behind the ego-cyclist.

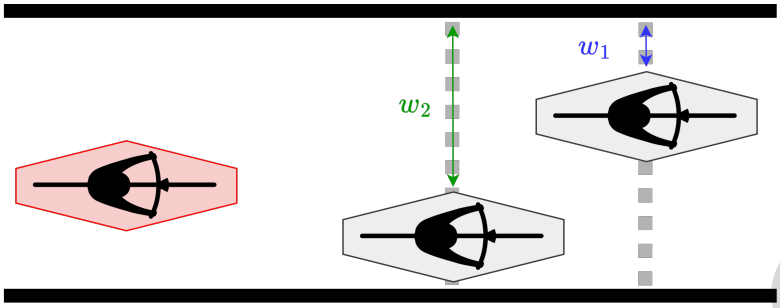

Figure 6. *Searching behavior for overtaking lateral space (green arrow: lateral space that is wider than the required safety region width, blue arrow: insufficient lateral space for overtaking)*

In SUMO, the sublane model divides a lane into multiple sublanes based on the *lateral resolution*, the width of a sublane, as illustrated in Figure 7. The lateral position of a bicycle is located at the center of one of the sublanes, while the width of a bicycle may occupy more than one sublane. In this work, a sufficiently small *lateral resolution* is used so that the model can be approximated as a non-lane-based model. The chosen value will be introduced in the next section.

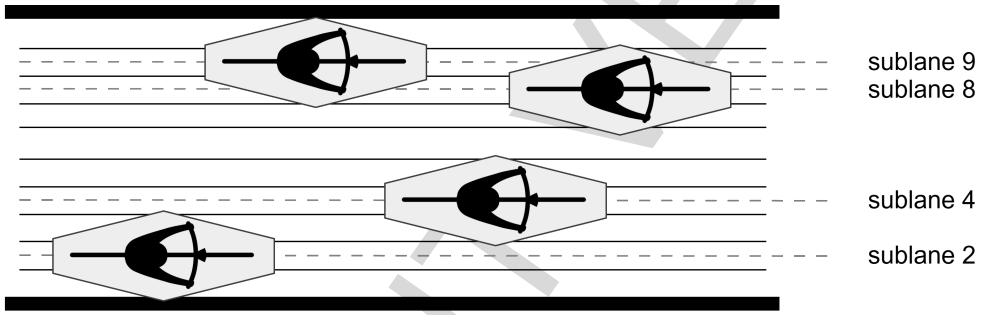

Figure 7. *Sublane model in SUMO (Example: Dividing a bicycle lane into ten sublanes with bicycles located on subalnes 2, 4, 8, and 9)*

The lateral movement distance determined in the mental-layer would be executed through the sublane-changing behavior by finding the closest (target) sublane after the lateral movement.

2.5 Physical-layer movements

Following the action and lateral movement distance decided in the mental-layer, the longitudinal acceleration would be subsequently computed in the physical layer. It is determined based on the distance and relative speed to the longitudinal leaders within the look-ahead distance that overlap with the ego-cyclist in the lateral plane. As shown in Figure 8, two of the three cyclists in front of the ego-cyclist are possible leaders, which would be considered for the calculation of longitudinal dynamics.

In the case of stopping, the deceleration depends on the distance to the stop line. The fundamental kinematic equation is applied, as written in Equation 3. Once the gap is smaller than a buffer threshold, the emergency braking is triggered to ensure that the cyclist would come to a standstill immediately.

$$a_{i+1} = \frac{-v_i^2}{2 \cdot (s_i - s^{\min} - s_b)} \tag{3}$$

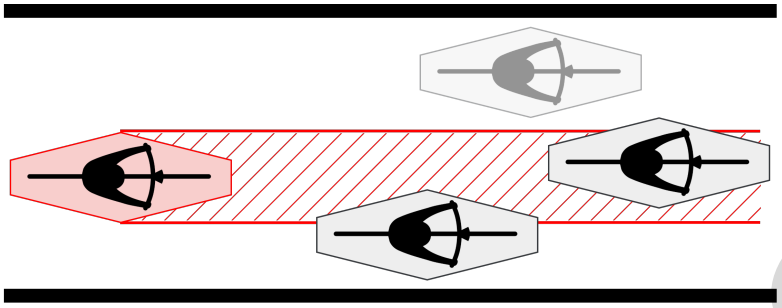

Figure 8. *Possible leaders (laterally overlapping with the ego-cyclist)*

In Equation 3, v_i denotes the current speed. s_i is the distance to the stop line, s^{min} indicates the minimum gap, while s_b is a buffer distance that must be considered due to the reaction time lag, which is explained in the next section.

If the cyclist does not aim to stop, the longitudinal acceleration is determined using IDM, as given in Equation 4, which is also the default option for bicycles in SUMO at the moment.

$$a_{i+1} = a^{\text{max}} \cdot [1 - (\frac{v_i}{v_{\text{des}}})^{\delta} - (\frac{s^*}{s_i})^2] \tag{4}$$

$$s^* = s^{\text{min}} + \max(0, l_{\text{safety}} - \frac{l_{\text{bic}}}{2} + s_b + \frac{v_i \Delta v_i}{2\sqrt{a^{\text{max}}|a^{\text{min}}|}}) \tag{5}$$

The maximum acceleration a^{max} and deceleration a^{min} are used in IDM. v_{des} denotes the desired speed of the ego-cyclist. δ is an IDM coefficient, which is usually set to 4. The desired dynamical gap s^* is defined in Equation 5. It depends on the SR length l_{safety}, the length of a bicycle l_{bic}, and the relative speed to the leader Δv_i. The buffer distance s_b is applied again to avoid collisions.

When queueing or conducting other actions without lateral movement, the ego-cyclist would simply adjust its acceleration based on IDM to align its longitudinal dynamics with the direct leader. In uninterrupted flow conditions, in particular, cyclists are believed to be able to anticipate downstream disturbances by looking at more than one leader. Hence, the ego-cyclist would examine all the accelerations computed based on the conditions with regard to all longitudinal leaders in the look-ahead distance and execute the most restricting value.

3. SUMO integration

This section explains how the proposed model is implemented in SUMO and all the necessary changes to the SUMO setup.

3.1 Parameters and simulation configuration

To disable the original cycling behavior in SUMO, we modify the speed mode and completely turn off the lane change mode through TraCI for every bicycle upon their entry

into the network. Finally, to switch on the sublane model environment, the *lateral resolution* is set to 0.1 m in the SUMO configuration so that the non-lane-based model logic can be applied.

Several vehicle type (vType) parameters need to be changed for bicycles to further enable the proposed model to run in SUMO. The width of a bicycle is set to 0.35 m, this covers only the width of the bicycle frame itself as cyclsits' arm span is considered by the unique gap calculation approach. The minimum longitudinal gap *minGap* and the minimum lateral gap *minGapLat* are set to 0 m so that collision detection based on the original rectangular shape representation is disabled.

The default lateral acceleration is 1.0 m/s^2 in the SL2015 lane-changing model in SUMO. This is applied to all vehicle types without the distinction between cars and two-wheelers, while we believe that a lower value should be used for bicycles. However, there is still little understanding on the lateral dynamics of bicycle movements in the literature. In this work, it is first set to 0.5 m/s^2. The value still needs to be carefully calibrated by analyzing empirical trajectories.

3.2 Decision-making frequency and reaction time lag

To ensure simulation accuracy and account for human factors, a simulation step size of 0.25 s is used by setting the *step-length* value. However, in reality, cyclists cannot generate movement decisions every 0.25 s, nor are car drivers. Therefore, an action step length of 0.5 s is applied, which means that cyclists only generate a new decision by calling the model every two simulation steps. In between two decision steps, cyclists move according to the previous decision.

The reaction time lag, which is not explicitly implemented in SUMO, is also considered for cyclists in this model. The decision made at every decision step would be stored and executed 0.5 s (two simulation steps) later. This is why a buffer term, as shown in Equation 6, must be applied to the gap when calculating the longitudinal acceleration to ensure that the simulation is collision-free. It is determined based on the hypothesis that cyclists would continue moving with their current acceleration a_i and speed v_i for the duration of a reaction time lag t^{react} before the decided action is performed.

$$s_b = v_i \cdot t^{\text{react}} + \frac{1}{2} \cdot \max(a_i, 0) \cdot (t^{\text{react}})^2 \tag{6}$$

Besides the buffer distance due to the reaction time lag, extra buffer needs to be included for the stopping and queueing actions to avoid passing the stop line and collision with leaders.

3.3 TraCI commands

The state variables of every individual bicycle, e.g., position, speed, acceleration, located lane, and signal phase, at every simulation step are obtained through multiple TraCI value retrieval functions.

Two TraCI vehicle state changing functions, `changeSublane` and `setSpeed`, are called to control cyclists' operational-level behavior, each corresponding to the lateral movement distance and longitudinal acceleration determined by the model in the mental- and physical-layers, respectively.

After the reaction time lag for each decision step, the `changeSublane` function executes the lateral movement with the default maximum lateral acceleration in the following time steps until the cyclist reaches the desired lateral position. On the other hand, at every time step, the longitudinal speed value for the `setSpeed` function is calculated using the current longitudinal speed of the ego-cyclist and the acceleration determined in the last decision step.

4. Model verification

A test scenario of a 2.5-meter-wide signalized bicycle lane is designed to verify the proposed model and its implementation in SUMO. The simulation period is one hour, while the inflow demand gradually increases to the capacity so that microscopic behavior in various traffic regimes can be observed.

To examine the model performance in difficult scenarios with great behavioral heterogeneity, the desired speed distribution has a standard deviation of 1.34 m/s, while the mean value is 5.24 m/s according to the findings in Kutsch et al. [18]. The inflow demand is large so that there are long queues before the stop line and the queueing behavior can be observed. Table 1 summarizes the unique cycling behavioral parameters that must be defined when using this model. Each parameter reflects an intuitively interpretable physical property, which facilitates easy model tuning. It should be noted that the parameter values are chosen in a way that collision is avoided after several trial simulation runs. Some of them can be customized or calibrated according to the simulation requirement, while there are a few that are recommended to remain unchanged to avoid unexpected simulation failure.

In the simulation test, there is no collision if there is no reaction time lag and decisions are made at every 0.25 s time step. When both the action step length and the reaction time lag are set to 0.5 s, collisions can be avoided by setting the residual gap threshold and distance buffers as in Table 1. Emergency brakings are mostly caused by the sudden change of a signal phase from green to yellow. It is also worth mentioning that different settings of parameters related to speed and acceleration could result in different outcomes.

With the sublane setup, the default SUMO simulation produces a multi-sublane bicycle queue with a uniform longitudinal gap between bicycles, as shown in the plot on the left in Figure 9. In contrast, staggered queue formations can be observed on a relatively wide bicycle lane when using the proposed model, as shown in the right plot. In addition, unlike the car-like deterministic queue, the various longitudinal and lateral gaps demonstrate that the proposed model introduces stochasticity into cyclists' queueing behavior. It is worth mentioning that the hexagonal shape of bicycles cannot be well-presented in the GUI as it is restricted by SUMO. Hence, several hexagonal shapes are drawn manually in the plot to demonstrate the staggered queue formation.

The simulated queue formation exhibits great similarity to the empirical queue formation shown in Figure 10. This shows that the hexagonal shape is a proper approximation of cyclists and verifies the functionality of the queueing behavior implemented in the model. Still, the simulated jam density in the simulated queue seems to be larger than the observed jam density in the empirical queue. This can be solved by calibrating the residual gap threshold, which is outside of the scope of the present work.

Table 1. *Model-specific parameters*

Parameter	Value	Meaning or purpose
gray!15 Changable		
SR length coefficient α	1.0	Determine the SR length, which can also be known as the minimum headway
SR width coefficient β	0.06	Determine the SR width
Maximum SR width δ^{max}	0.4 m	Constrain the SR width
Speed difference threshold ϵ	0.5 m/s	Determine the slow cyclists and required width for overtaking
Look-ahead distance	25 m	Cyclists downstream within this range are considered in the decision-making.
Look-back distance	10 m	Cyclists upstream within this range are considered in the decision-making.
Minimum TTC	5.0 s	Predictions are made for all future time steps within this range to avoid collisions.
Low speed threshold v_{low}	0.5 m/s	Threshold to define if the cyclist is in the low-speed mode
Discharge duration	5.0 s	The period of time a cyclist stays in the discharging mode to restrict any lateral movement
gray!15 Fixed		
Action step length	0.5 s	Decision-making frequency
Reaction time lag	0.5 s	Time lag for performing the action determined
Residual gap threshold g_{res}	1.0 m	Threshold determining if the residual gap in the standstill mode is short enough
Queueing distance buffer	0.25 m	Additional distance buffer to perform strong deceleration and avoid collisions when queueing
Stopping distance buffer	1.5 m	Additional distance buffer to perform strong deceleration and avoid passing the stop line when stopping

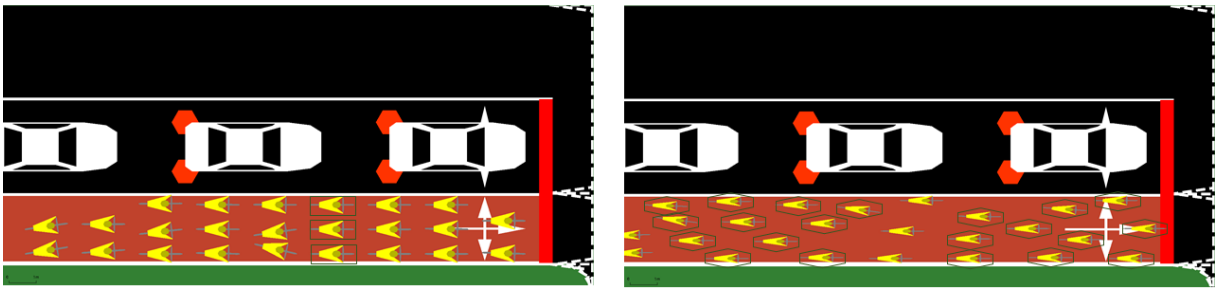

Figure 9. *Queue formations on a 2.5-m-wide bicycle lane (left: default SUMO setup with rectangular-shaped bicycles, right: the proposed model with hexagonal-shaped bicycles)*

The queue formations are also tested on different lane widths, 1.0, 1.5, and 2.0 m, as shown in Figure 11. The number of bicycles that can be accommodated in a unit length decreases when the lane width narrows. On a 1.0-m-wide lane, cyclists show a nearly single-file queue formation.

We further quantitatively investigate the efficiency of bicycle flow in every lane width by analyzing the maximum flow with an aggregation period of five minutes and the jam density by placing a 10-m long induction loop detector (E1) 10 m before the stop line. By making sure that the flow near the stop line is always saturated, the maximum flow

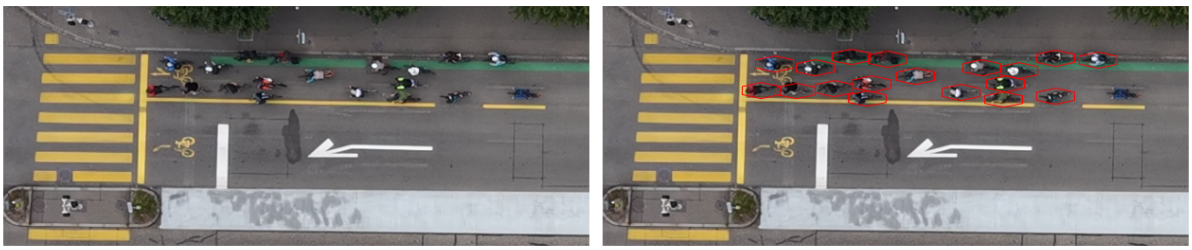

Figure 10. *Empirical queueing behavior on a 2.5-m-wide bicycle lane on Baslerstrasse in the city of Zurich (left: original image, right: image with queueing cyclists marked)*

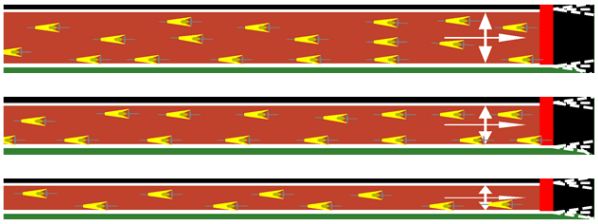

Figure 11. *Queue formations on other lane widths (top: 2.0 m, middle: 1.5 m, bottom: 1.0 m)*

can also be regarded as the interrupted flow capacity, or queue discharge rate. As shown in Table 2, the capacity of a 1.5-m wide lane is significantly larger than a 1.0-m wide lane. This is because cyclists can queue in parallel when the lane width is greater than 1.0 m. The quasi-multi-lane characteristic improves the capacity. However, the capacity gain becomes marginal from 1.5 m to 2.0 m as the situations of three cyclists queueing in parallel are still rare on a 2.0-m wide lane. A relatively large increase can be seen again when the lane width increases to 2.5 m. On the other hand, the jam density grows steadily as the lane width becomes wider. A higher jam density indicates a lower probability of queue spillback toward upstream bicycle lanes, mitigating the propagation of congestion in a network.

Table 2. *Capacities and jam densities*

	Lane width [m]			
	1.0	**1.5**	**2.0**	**2.5**
Capacity [bic/h]	1680	3216	3936	4752
Jam densities [bic/km]	413.8	698.3	836.2	1086.2

In general, the simulation test shows that the bicycle flow efficiency is improved as the lane width increases. This verifies that the proposed model produces different aggregated traffic performance in different lane widths according to its lateral movement logic. However, there is still a lack of understanding of the true cycling behavior on a wide bicycle lane. It has been empirically observed that cyclists may not utilize lateral space as efficiently as in a relatively narrow lane. We speculate that cyclists exhibit different lateral behaviors in different lane widths due to their safety perception. This suggests that different safety region parameters should be used in different lane widths. Empirical trajectory data are required to validate this hypothesis and help develop a realistic lateral movement behavior for bicycle flow.

5. Conclusions and future plan

This work develops a non-lane-based bicycle traffic simulation model that mimics cyclists' decision-making process when riding on a bicycle lane and implements it into SUMO. Unlike the default bicycle simulation function in SUMO at the moment, the model introduces the hexagonal representation of cyclists, enabling the staggered queue formation. It is an extension of the model proposed by Brunner et al. [12] with the ability to let cyclists (1) react to traffic signals in interrupted flow conditions (2) actively avoid collisions through prediction and (3) queue efficiently by performing a space finding behavior. Compared to the laterally-continuous bicycle movement model based on the TTC maximization principle proposed by Falkenberg et al. [13] and later adopted in PTV Vissim, more detailed behavior is designed for various actions and surrounding conditions. In addition, (4) the model incorporates human factors by considering decision-making frequency and reaction time lag, making the model more realistic and allowing it to be used for cycling safety assessment [19].

In comparison to *CyclistsModel* that computes cyclists' position at every simulation step, this model outputs two variables, longitudinal acceleration and lateral movement distance, at every decision step and interacts with the sublane model in SUMO through two TraCI vehicle state changing functions. By maintaining more SUMO setup, we improve the flexibility of the model for applications in the simulation of large-scale urban road networks.

Still, many functionalities are being developed to enable the application of the model at network-level, such as strategic alignment behavior to bottlenecks and downstream turning. Other add-ons are also required to enable the simulation of yielding behavior within unsignalized intersections.

Future work will also calibrate the model parameters using bicycle trajectory data collected with drones in the BikeZ-ETH dataset [20], [21]. The approach of defining groups of cyclists with different dynamics parameters, as introduced in Karakaya et al. [22], will be considered. The acceleration/deceleration profiles at the start of the movement and when approaching a red light also need to be carefully calibrated [18], [23], [24]. Based on the empirical findings, the inter-dependencies between variables could also be captured. The reproduced cycling traffic flow dynamics could then be validated by analyzing fundamental diagrams to ensure that the model is applicable in every traffic regime.

Data availability statement

The current work does not yet rely on any data. The BikeZ-ETH trajectory dataset will soon be made available and can be accessed here: https://bikez.ethz.ch/.

Underlying and related material

The Python codes and SUMO packages of the test scenarios will be made available here: https://github.com/YCNi/BikeZ.git

We promote the principles of open and reproducible science. In line with this commitment, our work aligns with the goals of the Reproducible Research in Transportation (RERITE) Working Group, which advocates transparency, reproducibility, and data

sharing in transportation research. More information about the working group is available at https://www.rerite.org/.

Author contributions

Ying-Chuan Ni: Conceptualization, Methodology, Software, Visualization, Writing – original draft

Thomas Ramseier: Methodology, Software, Writing – review & editing

Junzhe Cao: Conceptualization, Writing – review & editing

Anastasios Kouvelas: Methodology, Supervision, Writing – review & editing

Michail A. Makridis: Methodology, Funding acquisition, Supervision, Writing – review & editing

Competing interests

The authors declare that they have no competing interests.

Funding

This work is part of the “BikeZ: Model Suite for Mass Cycling as a Service Simulation” Innovation project supported by Innosuisse (grant agreement: 123.077 IP-SBM).

Acknowledgements

The authors would like to thank Univ.-Prof. Dr.-Ing. Heather Kaths at the Chair of Bicycle Traffic, Bergische Universität Wuppertal, other participants in the first Cyclist Behavior Modelling Workshop at Technische Universität München, and anonymous reviewers for the insightful feedback.

References

[1] A. Lanvin, J. Charléty, G. Ferreol, *et al.*, “How to create a sustainable growth in bicycle traffic? The case of Paris,” *Journal of Cycling and Micromobility Research*, vol. 5, p. 100 081, Sep. 2025, ISSN: 29501059. DOI: 10.1016/j.jcmr.2025.100081.

[2] H. Twaddle, T. Schendzielorz, and O. Fakler, “Bicycles in Urban Areas,” *Transportation Research Record: Journal of the Transportation Research Board*, vol. 2434, no. 1, pp. 140–146, Jan. 2014, ISSN: 0361-1981. DOI: 10.3141/2434-17.

[3] D. Ton, A. Gavriilidou, Y. Yuan, F. Schneider, S. Hoogendoorn, and W. Daamen, “Modeling of cycling behavior,” in 2022, pp. 159–186. DOI: 10.1016/bs.atpp.2022.06.001.

[4] Y.-C. Ni, M. A. Makridis, and A. Kouvelas, “Bicycle as a traffic mode: From microscopic cycling behavior to macroscopic bicycle flow,” *Journal of Cycling and Micromobility Research*, vol. 2, p. 100 022, Dec. 2024, ISSN: 29501059. DOI: 10.1016/j.jcmr.2024.100022.

[5] M. J. Wierbos, V. L. Knoop, F. S. Hänseler, and S. P. Hoogendoorn, “Capacity, Capacity Drop, and Relation of Capacity to the Path Width in Bicycle Traffic,” *Transportation Research Record: Journal of the Transportation Research Board*, vol. 2673, no. 5, pp. 693–702, May 2019, ISSN: 0361-1981. DOI: 10.1177/0361198119840347.

[6] P. A. Lopez, E. Wiessner, M. Behrisch, *et al.*, “Microscopic Traffic Simulation using SUMO,” in *2018 21st International Conference on Intelligent Transportation Systems (ITSC)*, IEEE, Nov. 2018, pp. 2575–2582, ISBN: 978-1-7281-0321-1. DOI: 10.1109/ITSC.2018.8569938.

[7] G. Grigoropoulos, S. A. Hosseini, A. Keler, *et al.*, “Traffic Simulation Analysis of Bicycle Highways in Urban Areas,” *Sustainability*, vol. 13, no. 3, p. 1016, Jan. 2021, ISSN: 2071-1050. DOI: 10.3390/su13031016.

[8] E. J. Fulton, Y.-C. Ni, and A. Kouvelas, “Impact of radical bike lane allocation on bi-modal urban road network traffic performance: A simulation case study,” *Case Studies on Transport Policy*, vol. 22, p. 101 583, Dec. 2025, ISSN: 2213624X. DOI: 10.1016/j.cstp.2025.101583.

[9] A. Roosta, H. Kaths, M. Barthauer, J. Erdmann, Y.-P. Flötteröd, and M. Behrisch, “State of Bicycle Modeling in SUMO,” *SUMO Conference Proceedings*, vol. 4, pp. 55–64, Jun. 2023, ISSN: 2750-4425. DOI: 10.52825/scp.v4i.215.

[10] H. Kaths and A. Roosta, “Framework for Simulating Cyclists in SUMO,” *SUMO Conference Proceedings*, vol. 4, pp. 105–113, Jun. 2023, ISSN: 2750-4425. DOI: 10.52825/scp.v4i.219.

[11] H. Kaths, “A movement and interaction model for cyclists and other non-lane-based road users,” *Frontiers in Future Transportation*, vol. 4, Oct. 2023, ISSN: 2673-5210. DOI: 10.3389/ffutr.2023.1183270.

[12] J. S. Brunner, Y.-C. Ni, A. Kouvelas, and M. A. Makridis, “Microscopic simulation of bicycle traffic flow incorporating cyclists’ heterogeneous dynamics and non-lane-based movement strategies,” *Simulation Modelling Practice and Theory*, vol. 135, p. 102 986, Sep. 2024, ISSN: 1569190X. DOI: 10.1016/j.simpat.2024.102986.

[13] G. Falkenberg, A. Blase, T. Bonfranchini, *et al.*, “Bemessung von Radverkehrsanlagen unter verkehrstechnischen Gesichtspunkten, Berichte der Bundesanstalt für Straßenwesen,” Tech. Rep., 2003.

[14] A. Gavriilidou, W. Daamen, Y. Yuan, and S. Hoogendoorn, “Modelling cyclist queue formation using a two-layer framework for operational cycling behaviour,” *Transportation Research Part C: Emerging Technologies*, vol. 105, pp. 468–484, Aug. 2019, ISSN: 0968090X. DOI: 10.1016/j.trc.2019.06.012.

[15] M. Wierbos, V. Knoop, R. Bertini, and S. Hoogendoorn, “Influencing the queue configuration to increase bicycle jam density and discharge rate: An experimental study on a single path,” *Transportation Research Part C: Emerging Technologies*, vol. 122, p. 102 884, Jan. 2021, ISSN: 0968090X. DOI: 10.1016/j.trc.2020.102884.

[16] G. Grigoropoulos, H. Kaths, and F. Busch, “Introducing the Effect of Bicyclist Stabilization Control in Microscopic Traffic Simulation,” in *2019 IEEE Intelligent Transportation Systems Conference (ITSC)*, IEEE, Oct. 2019, pp. 1373–1378, ISBN: 978-1-5386-7024-8. DOI: 10.1109/ITSC.2019.8916880.

[17] PTV Group, *PTV Vissim: Multimodal Traffic Simulation Software*, 2026. [Online]. Available: https://www.ptvgroup.com/en/products/ptv-vissim.

[18] A. Kutsch, L. Kessler, and K. Bogenberger, “Analyzing Bicycle Riding Characteristics Based on Naturalistic Urban Drone Observations: Free Riding, Following Behavior, and Overtaking Maneuvers,” *Transportation Research Record: Journal of the Transportation Research Board*, vol. 2679, no. 9, pp. 900–914, Sep. 2025, ISSN: 0361-1981. DOI: 10.1177/03611981251341354.

[19] C. M. Konrad, A. Dabiri, F. Schulte, J. K. Moore, and R. Happee, “Cycling safety assessment in microscopic traffic simulation: A review and methodological framework,” *Trans-*

portation Research Interdisciplinary Perspectives, vol. 34, p. 101 734, Nov. 2025, ISSN: 25901982. DOI: 10.1016/j.trip.2025.101734.

[20] BikeZ-ETH, *BikeZ-ETH: An openly available bicycle trajectory dataset & a mass cycling traffic flow simulation tool*, 2026. [Online]. Available: https://bikez.ethz.ch/.

[21] K. Riehl, S. K. El-Baklish, Y.-C. Ni, A. Kouvelas, and M. A. Makridis, "BikeZ-ETH – A Mass-Cycling Trajectory Dataset from a Controlled Experiment," *Scientific Data*, Apr. 2026, ISSN: 2052-4463. DOI: 10.1038/s41597-026-07247-7.

[22] A.-S. Karakaya, I.-A. Stef, K. Köhler, J. Heinovski, F. Dressler, and D. Bermbach, "Achieving realistic cyclist behavior in SUMO using the SimRa dataset," *Computer Communications*, vol. 205, pp. 97–107, May 2023, ISSN: 01403664. DOI: 10.1016/j.comcom.2023.04.015.

[23] H. Twaddle and G. Grigoropoulos, "Modeling the Speed, Acceleration, and Deceleration of Bicyclists for Microscopic Traffic Simulation," *Transportation Research Record: Journal of the Transportation Research Board*, vol. 2587, no. 1, pp. 8–16, Jan. 2016, ISSN: 0361-1981. DOI: 10.3141/2587-02.

[24] A. Schöckel, L. Kessler, and K. Bogenberger, "Bicycle queues at signalized intersections — A drone-based empirical analysis of headways, saturation flows, and time losses," *Journal of Cycling and Micromobility Research*, vol. 8, p. 100 117, Jun. 2026, ISSN: 29501059. DOI: 10.1016/j.jcmr.2026.100117.